

Article 4

Geological modelling for investigating CO₂ emissions in Florina Basin, Greece

Tasianas, A., N. Koukouzas, V. Gemeni, D. Alexopoulos and C. Vasilatos

Open Geosciences, 7(1), 465–489 (2015)



Research Article

Open Access

Nikolaos Koukouzas, Alexandros Tasianas*, Vasiliki Gemeni, Dimitrios Alexopoulos, and Charalampos Vasilatos

Geological modelling for investigating CO₂ emissions in Florina Basin, Greece

DOI 10.1515/geo-2015-0039

Received September 11, 2014; accepted January 10, 2015

Abstract: This paper presents an investigation of naturally occurring CO₂ emissions from the Florina natural analogue site in Greece. The main objective was to interpret previously collected depth sounding data, convert them into surfaces, and use them as input to develop, for the first time, 3D geological models of the Florina basin. By also locating the extent of the aquifer, the location of the CO₂ source, the location of other natural CO₂ accumulations, and the points where CO₂ reaches the surface, we were able to assess the potential for CO₂ leakage. Geological models provided an estimate of the lithological composition of the Florina Basin and allowed us to determine possible directions of groundwater flow and pathways of CO₂ flow throughout the basin.

Important modelling parameters included the spatial positions of boundaries, faults, and major stratigraphic units (which were subdivided into layers of cells). We used various functions in Petrel software to first construct a structural model describing the main rock boundaries. We then defined a 3D mesh honouring the structural model, and finally we populated each cell in the mesh with geologic properties, such as rock type and relative permeability.

According to the models, the thickest deposits are located around Mesochorion village where we estimate that around 1000 m of sediments were deposited above the basement. Initiation of CO₂ flow at Florina Basin could have taken place between 6.5 Ma and 1.8 Ma ago. The NE-SW oriented faults, which acted as fluid flow pathways, are still functioning today, allowing for localised leakage at the surface. CO₂ leakage may be spatially variable and episodic in rate. The episodicity can be linked to the timing of Almopia volcanic activity in the area.

Keywords: CO₂ seepage; aquifer; groundwater flow; sedimentary basin; Neogene

Nikolaos Koukouzas, Vasiliki Gemeni, Dimitrios Alexopoulos: Centre for Research & Technology Hellas, Chemical Processes and Energy Resources Institute (CERTH/CPERI), 15125, Athens, Greece

© 2015 N. Koukouzas *et al.*, licensee De Gruyter Open.

This work is licensed under the Creative Commons Attribution-NonCommercial-NoDerivs 3.0 License.

The article is published with open access at www.degruyter.com.

1 Introduction

Natural analogues of CO₂ emissions all over the world [1] provide valuable clues into the role nature plays in keeping CO₂ trapped underground for geologically significant amounts of time [1]. Many of these naturally occurring accumulations, whether they are CO₂-rich waters at depth or CO₂-rich waters at the surface in the form of springs, dry CO₂ gas vents, or CO₂ gas accumulations, have been shown to retain CO₂ for longer time spans than the retention periods under consideration for industrial CO₂ storage [1]. Although a lot of work has been previously carried out on natural CO₂ deposits [2–4], their scientific study still remains at an early phase [5].

CO₂ gas accumulations can occur in Cenozoic extensional basins (e.g. the back-arc Pannonian Basin and the Florina-Ptolemais-Aminteo graben system) [1]. Natural analogues, such as the CO₂ seepage in the Florina Basin in NW Greece (see red asterisk, Figure 1a), provide information on both the short- and long-term causes of CO₂ leakage and effects on the surrounding environment [6]. Other sites, such as various Mesozoic and Palaeozoic basins that were subject to Cenozoic tectonism (e.g. the Triassic to Jurassic Southeast Basin of France and sub-basins within the Southern Permian Basin in Saxo-Thuringia, Germany) can also host CO₂ accumulations [1].

The study area is part of the Florina Basin (Figure 1a) and covers 487.2 km². (See the red polygon corresponding to the study area coverage [Figure 1a], the polygon corresponding to the study area outline [Figure 1b] and the section on model characteristics below). The wider NNW-SSE

***Corresponding Author: Alexandros Tasianas:** Centre of Excellence for Arctic Gas Hydrates, Environment and Climate (CAGE), Department for Geology, Arctic University of Norway, Tromsø, N-9037, Norway, E-mail: corresponding author: alexandros.tasianas@uit.no

***Corresponding Author: Alexandros Tasianas:** Centre for Research & Technology Hellas, Chemical Processes and Energy Resources Institute (CERTH/CPERI), 15125, Athens, Greece

Charalampos Vasilatos: Department of Economic Geology and Geochemistry, Faculty of Geology and Geoenvironment, National & Kapodistrian University of Athens, 15724, Athens, Greece

oriented graben in which the Florina Basin is located is filled with a thick sedimentary succession. The lower part of the basin constitutes the plain of Florina, which has an average altitude of around 620 m and an area of around 220 km² (Figure 1b) [7]. The edges of the basin are characterized by mountain highs, reaching a peak of 1212 m in the SW region of the study area (Figure 1b).

Little research has been conducted in the Florina Basin. Thus, the problem being considered here requires us to develop a better understanding of how the stratigraphy and the structure vary laterally and vertically across the Florina Basin. Previous work has mainly elaborated on a hydrogeological study of the basin [7] in order to evaluate ground water deposits to be exploited for development of agricultural areas in the region. Geological, hydrogeological and hydrolithological mapping was previously performed in the entire hydrogeological Florina Basin [7], as well as an inventory of the water points.

The aims of the present study are therefore to visualise in 3D the entire Florina Basin through the development of 3D geological models, and thus better understand how the naturally occurring CO₂ present in the area could migrate through the sediments to reach the surface. One of the main reasons for selecting the study area as a suitable analogue for commercial CO₂ storage sites is the fact that there is a large quantity of CO₂ that dissolves in the Florina aquifers.

This succession represents, together with its lignite deposits, the main autochthonous source of fossil combustible in Greece, with about 50% of national stationary CO₂ emissions coming from this area [8]. Therefore, any CO₂ emission mitigation strategies developed and applied here would have a larger impact nationwide. Since the Florina Basin is a site of many CO₂ point sources, further study is warranted in order to assess its potential as a geological storage site. The Florina Basin thus represents not only an excellent site (Figure 1) for commercial exploitation of the CO₂ as an industrial gas, but it is also a good natural analogue for studying the impact of Carbon Capture and Storage (CCS) in general [9].

In order to better understand the Florina Basin (Figure 1a), we developed, for the first time, lithological and relative permeability models for the Florina site. To accomplish this, we used 1) formation top data from electromagnetic depth soundings that were carried out in the 1970s, 2) structural elements such as faults and any other information from boreholes that were drilled in the area, and 3) superficial evidence of CO₂ seepage [10]. This data improved our knowledge of the structure and fluid migration processes involved in natural CO₂ seepage. The results are used as an analogue for CO₂ leakage from reservoirs where

CO₂ has been injected, such as in the case of Snøhvit in the Barents Sea [11–14]. Such 3D models provide us with a better explanation of how the CO₂ migrates in the shallow subsurface, which leakage pathways it takes, and what timescales are involved in CO₂ leakage initiation and duration [15].

We focus on the geological characterisation of the Florina site (Figure 1) and the ascent of CO₂ from the geological reservoir, located in Neogene sandstones and conglomerates at 300 m depth below ground surface in the Mesochorion area [16], through the sedimentary strata and finally to the groundwater table. These processes are then compared and contrasted with the Snøhvit site, which has been the focus of previous research work [11–14, 17], and other sites worldwide.

2 Geological setting and Florina terrestrial site study area

2.1 Geological and stratigraphic setting

The Florina CO₂ field belongs to the Pelagonian tectonic zone of the internal Hellenides (Figure 2) [1, 18]. It is located in the NNW-SSE oriented Florina-Ptolemais-Aminteo graben system, a Cenozoic extensional basin in Northern Greece (Figures 1 and 2) [1, 18].

This NNW-SSE intramontane graben is composed of metamorphic rocks (Figures 2 and 3) [19, 20] and formed as a result of extensional stresses following the Alpine orogenesis [1, 18]. During the Late Miocene-Early Pliocene, the basin began to fill with terrestrial, fluvial and lacustrine deposits that reached a total thickness of up to 800-1000 m (Figures 2 and 3) [21, 22]. The sediment fill is surrounded by 1) carbonate rocks of the Pelagonian zone, mostly marbles which outcrop mainly in the SE region of the study area and 2) metamorphic rocks outcropping in the NE of the basin (Figures 2 and 3) [19]. The western side of the basin is predominantly comprised of high mountain masses (Figures 1b, 2 and 3) composed of schist, gneiss and other plutonic and metamorphic rocks [7, 20, 23]. The southern part of the basin is composed mainly of Neogene sediments (Figures 2 and 3) [7, 20].

Geological units in order from oldest (metamorphic basement) to youngest (alluvial deposits) are described below (Figures 2 and 3). All described units outcrop at the surface (Figure 2).

Figure 4 illustrates the relative permeability variation in the area. The permeability variation is represented in the form of qualitative permeability values ranging from

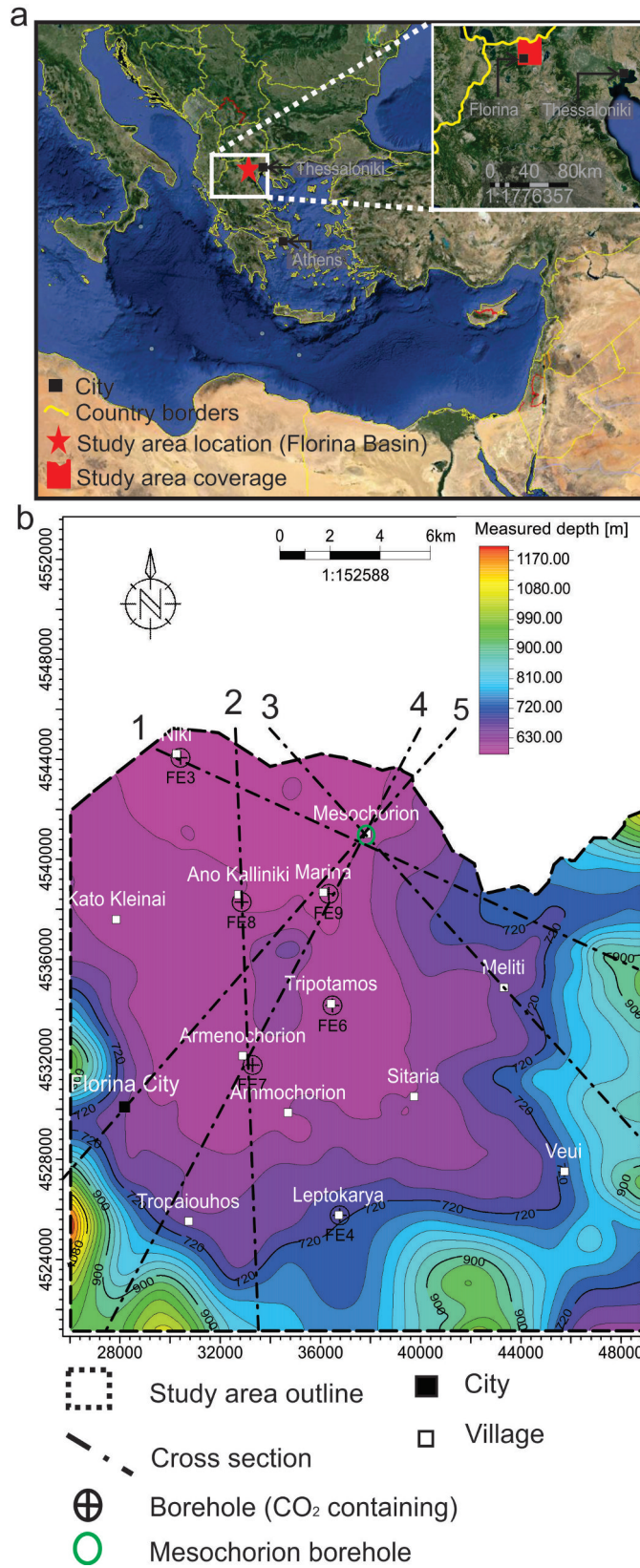


Figure 1: a) Study area location and geological model outline. b) Ground level surface within the extent of the geological model outline showing borehole and various cross section locations.

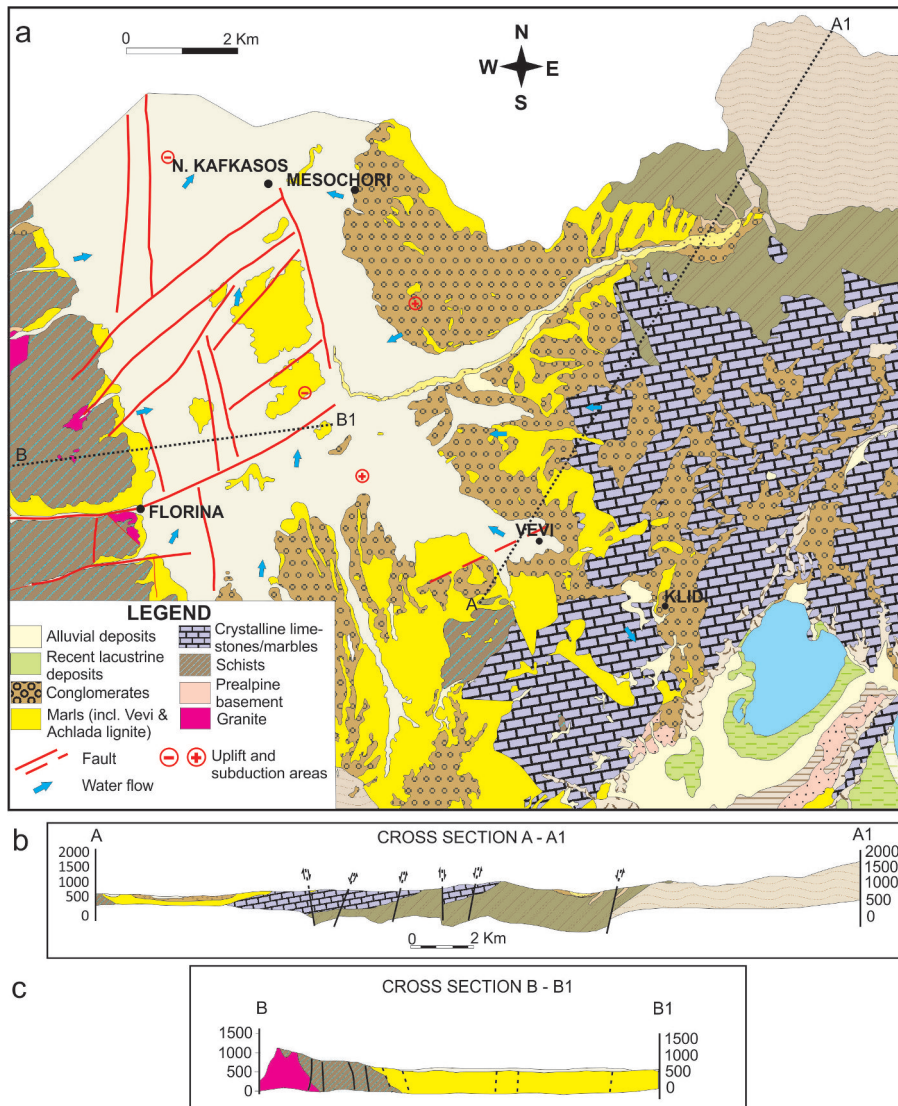


Figure 2: a) Geological map of the Florina Basin study area, containing both the lithological distribution and faults. b) and c) are representative cross-sections A-A1 and B-B1 respectively.

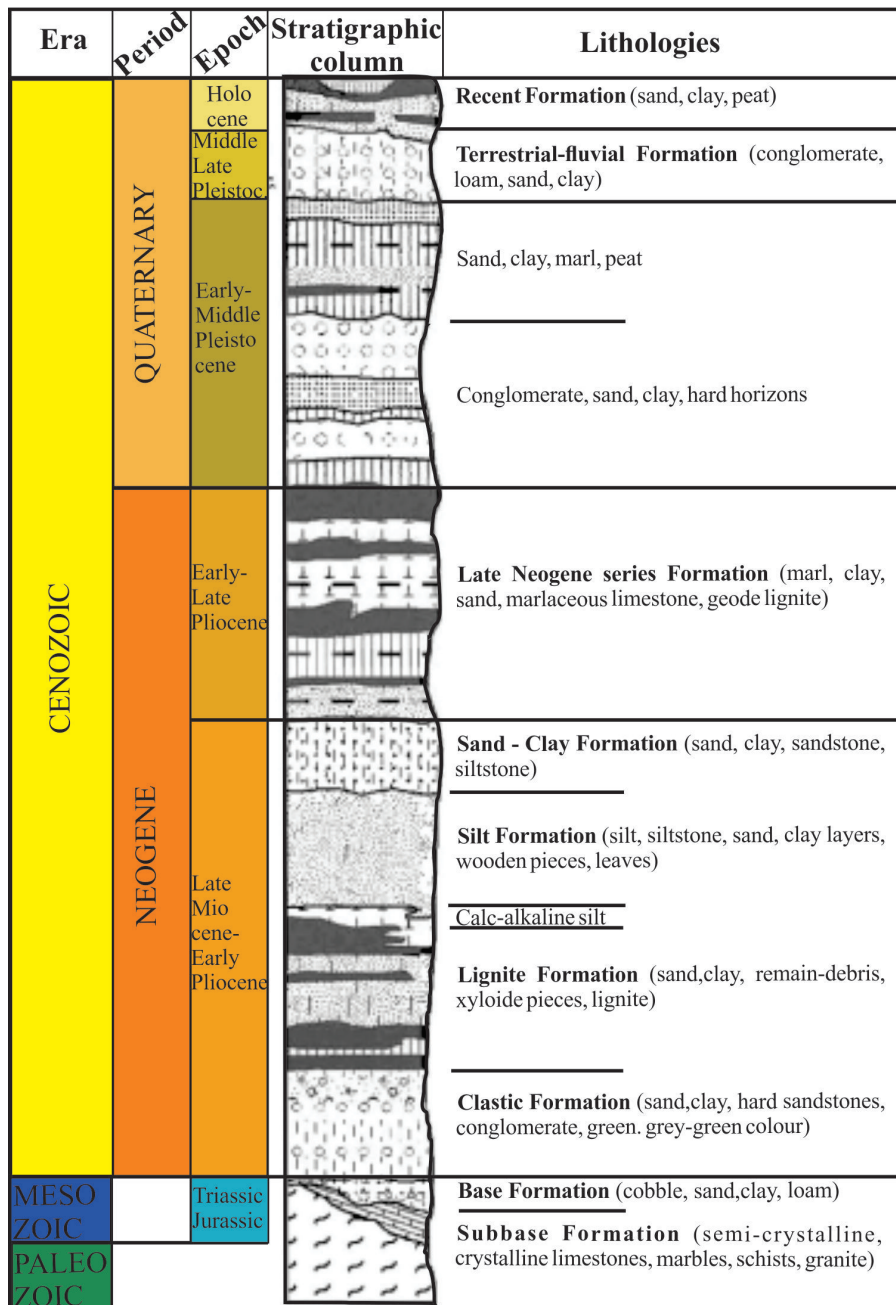


Figure 3: Synthetic stratigraphic column of the Florina-Ptolemais-Aminteo Graben system. (Figure modified from [21].

impermeable to very high permeability for the different units outcropping at the surface. Based on this map, we simplified the natural system by regrouping the values of the various units into 5 zones (the same 5 zones that were used in the model building process - see Section 3.2 below). For a detailed explanation of the methods used to determine the average permeability for each zone, see Section 3.2.

The metamorphic basement (Figures 2 and 3) consists of layers of schist, leptinites and gneiss with granitic intercalations and quartz dykes [20]. It is generally an impermeable unit but zones of low permeability can appear in areas where rocks are altered (Figure 4) [7].

On top of the metamorphic basement lies the thin, semi-crystalline limestones and marbles of the Pelagonian Nappe (Figures 2 and 3). These sediments are well bedded, karstified and often strongly fractured, thus explaining their high to very high permeability (Figure 4) [7].

As we move up the stratigraphic column, the next unit consists of Neogene marls and clays (Figures 2 and 3). They are characterised by fossiliferous marly limestones and marls alternating with clayey marls and clays (Figures 2 and 3) [20, 21]. The basic conglomerates of the Neogene are characterised by a permeability which is generally high (Figure 4) [7, 21]. Travertine, like the limestones of the Neogene, are of moderate and locally high permeability (Figure 4) [7]. Finally, the Pliocene lacustrine deposits consist of alternating layers of marls, sands, sandstones, conglomerates and marly schists [?]. They have a permeability which is generally moderate to high in areas where sands, sandstones, conglomerates and marly limestones prevail and low in areas where marl prevails (Figure 4). In the relative permeability model, an overall average relative permeability of moderate to high is attributed to the Neogene lithologies [7].

Overlying the Neogene marls and clays are the Pleistocene conglomerates, (Figures 2 and 3) which can be of two types in the study area. The first type consists mainly of various calcareous pebbles and a calcitic matrix, and the second type are associated with sandstones, sands and red clays of river torrential origin. This eluvial formation, on top of the Pliocene deposits, is characterised by medium to low permeability (Figure 4) [7]. When the amount of pebbles increases the permeability varies from moderate to locally high (Figure 4) [7]. We assign an overall moderate average permeability to the Pleistocene conglomerates.

The Holocene deposits are the youngest of all units that outcrop in the study area (Figures 2 and 3) and consist of alluvial deposits [21]. Clay silts, fine grained sands and pebbles are well mixed, giving the alluvial deposits a low

to medium permeability (Figure 4) [7]. In low areas of the basin, where terra rossa with pebbles prevails, the permeability is very low. The recent river torrential deposits, principally found along the branches of the hydrographic system, are characterised by deposits of generally high permeability (Figure 4) [7]. As these are only localised, we assign an overall low to moderate average permeability to the Holocene alluvial sediments.

2.2 Tectonic setting

The Florina Basin is a tectonic trench characterized by faults striking NNW-SSE (Figure 2) [7]. The area has been affected by 2 main tectonic phases: one in the Caledonian, which caused folding of the schist and created granitic intrusions, and a second more recent alpine phase, which formed the Pre-Pliocene trench of Florina [7, 24].

During the end of the Alpine phase and Early Miocene [21], intense tectonic faulting began in NW Greece [24]. Faults of NW-SE direction (Figure 2), created during this NE-SW Late Miocene extension [24, 25], resulted in the development of the Florina Basin [21].

The Pliocene formations of the basin can be generally described as monoclines with a strike of 20°–40°N and a dip towards the NW on the order of 15°–30° (Figure 2) [7]. A more recent tectonic phase also affected the Pliocene formations, creating rock-bursts of almost vertical dip and NNW-SSE and NE-SW strike [7].

The carbonate-rich springs and CO₂-rich gas vents observed throughout the Florina Basin [19] may be the result of a slow upwelling of magmatic, hydrothermal CO₂ along faults and fractures [22]. Gas leakage occurs as a series of isolated “spots” that are aligned in a general NE-SW direction, which parallels one of the main fault directions in the region. Thus, faults are thought to be important for CO₂ transport and upwelling (Figure 2)¹. Relatively low pH values were also observed along the major fault lines with a NE-SW direction (Figure 2)¹.

2.3 CO₂ gas source, accumulation and leakage

The CO₂ in the Florina Basin is volcanic in origin¹ [16]. CO₂ gas accumulation occurs in Miocene fluvial sandstones (Figures 2 and 3) [9, 23]. The vertically stacked reservoirs

¹ RISCs, Research into impacts and safety in CO₂ storage. 2012(No 4).

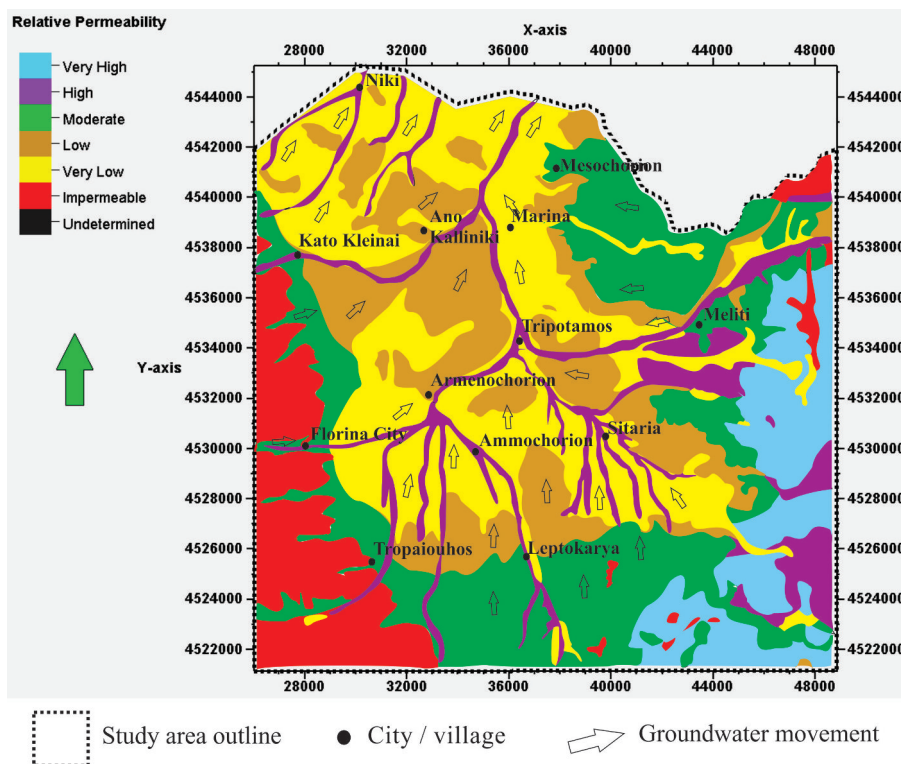


Figure 4: Hydrogeological map of the Florina Basin showing relative permeability for the various lithologies, hydrography and groundwater movement directions. (Figure modified from [7].)

are composed of limestone and sandstone units (with the upper unit at 300 m depth) capped by silts, marls and clays (Figures 2 and 3) [6, 23]. The Base formation, which appears at depths of 251 m to 548 m [16], contains the CO₂ accumulations, which are found in fine sands that mostly accumulated in a fluvial environment. CO₂ also occurs at different levels in the Mesozoic limestones (Figures 2 and 3) [18]. Local Florina cap rocks are comprised of clayey sediments [18]. The fluvial and alluvial fan environment that characterizes the Florina Basin is ideal for CO₂ storage [16]; any internal stratigraphic changes within this environment of sedimentation retain CO₂ and do not allow it to escape [16].

Natural CO₂ accumulations have been detected from depths of 296-338 m and 366-372 m below the surface [16]. These CO₂ accumulations lack an upper layer of fine minerals that could act as a cap rock [16]. Another four accumulations of CO₂ have also been detected at depths of 380-409 m below the surface, also characterised by an absence of an upper cap rock layer [16].

CO₂ leakage creates mineral springs and gas seeps in some places and/or gas bubbles in shallow wells in others [6, 19]. Geological features such as fractures and permeable cap rock provide a pathway for the slow CO₂ mi-

gration. The study area is also characterized by CO₂ vents and carbonate springs along rock discontinuities [18, 26]. This naturally produced CO₂ leaks to the surface in various locations. One such location was chosen for detailed biological and chemical research by RISCS, who conducted a semi-regional soil-gas and gas-flux survey in and around the site at Florina¹. Results showed that soil-gas CO₂ concentrations ranged from normal background values, less than 3%, up to highly anomalous values in the centre of gas vents, which reached almost 100% at 70 cm depth¹.

Natural leakage of CO₂ is a slow process that takes place along rock discontinuities [6]. With industrial leakage of CO₂, well blowout is considered an event that triggers leakage because the CO₂ uses the well as a pathway [6]. In Florina, however, CO₂ gas is found in soils at the surface and in water-filled pools around some wells where no blowout occurred [6].

Within the city of Florina there has been evidence of CO₂ reaching the ground surface. In areas where CO₂ has reached the surface, CO₂ has affected the vegetation (Figure 5). For example, the effect of CO₂ on the geomorphology of fields within the city can be clearly seen at a mineral water exploration well that was drilled there in order to locate the CO₂-rich mineral water (Figure 6) [10]: a small



Figure 5: Photo showing damaged pasture from natural CO₂ seeps in the Florina area [10].



Figure 6: Photo of a small lake created as a result of upward migration of naturally occurring CO₂ outside the casing of a mineral water exploration well drilled in the Florina area [10].

lake has been created (Figure 6) as a result of the upwards migration of naturally occurring CO₂ outside the casing of the mineral water exploration well [10].

The well was cased throughout with a steel tube, and well completion included the installation of a wellhead with a valve (Figure 6) [10]. CO₂ was detected along the well between depths of 97 m and 559 m. Once well completion activities were finished and while the valve of the wellhead was closed, CO₂ leakage was observed at a distance of 100 m from the well. There was an advancement of the CO₂ leakage towards the well at a later stage, which created a hole around the well with an area of more than 25 m² (5 × 5 m) and a depth of 50 m (Figure 6). The cement base used for the drill rig collapsed, and as a result a small lake was created, as illustrated in Figure 6. The quantity of CO₂ involved is not known but the fact that the borehole was destroyed illustrates that the quantity of CO₂ migrating to the surface was high enough to lead to the corrosion and destruction of the borehole. The natural CO₂ seeps have also damaged pastures in the area (Figure 5) [10].

3 Data and methods

3.1 Introduction

We identified a total of 150 measurement point locations within the boundaries of the study area (Figure 1) corresponding to boreholes or points where electrical soundings had been carried out in the early 1970s (Figures 7 and 8) [7]. The electrical sounding data collected at the time, which included formation top depths and presence of faults, were recorded on paper [7]. We transformed this data into points in 3D space in Petrel and used them for creating a database. We then used this “formation tops” database to construct the first geological model, consisting of a lithological model, a relative permeability model and a model of the aquifer background of the Florina Basin.

The geo-electrical depth soundings (Figure 7) [7] were positioned along geological trace profiles, as also shown by the map of electrical sounding point. For each depth sounding we located different formation tops (Table 1) and recorded the depths, measured from ground surface. Formation tops with the same names but with different endings (e.g. Sand M1 and Sand X) indicate the same lithological composition but correspond to lenses located in different locations of the basin or layers of the same composition but stratigraphically at different levels.

The depth sounding dataset covers the entire 487.2 km² area of the Florina Basin and corresponds to the area within the boundaries of the geological model (Figures 1, 7 and 8). The depth soundings were collected in July 1974 by Barringer Research Ltd. In 6 out of the 150 geo-electrical soundings, an analysis of the carbon dioxide and oxygen content on the ground water was also made (see Table 2 below and CO₂ containing wells in Figure 8). A well was also drilled in the Mesochorion area, as part of a previous study, (see well penetrating CO₂ accumulations in Figure 8) where we encountered CO₂ accumulations and thus the geological reservoir(s) for CO₂ in the basin [16].

3.2 Geological Model description

3.2.1 Geological zonation

We built a 5-zone geological model of the Florina Basin using Petrel software. The 5-zone model was comprised of the following zones: a metamorphic basement, a Pelagorian Nappe (marbles and limestones), Neogene deposits

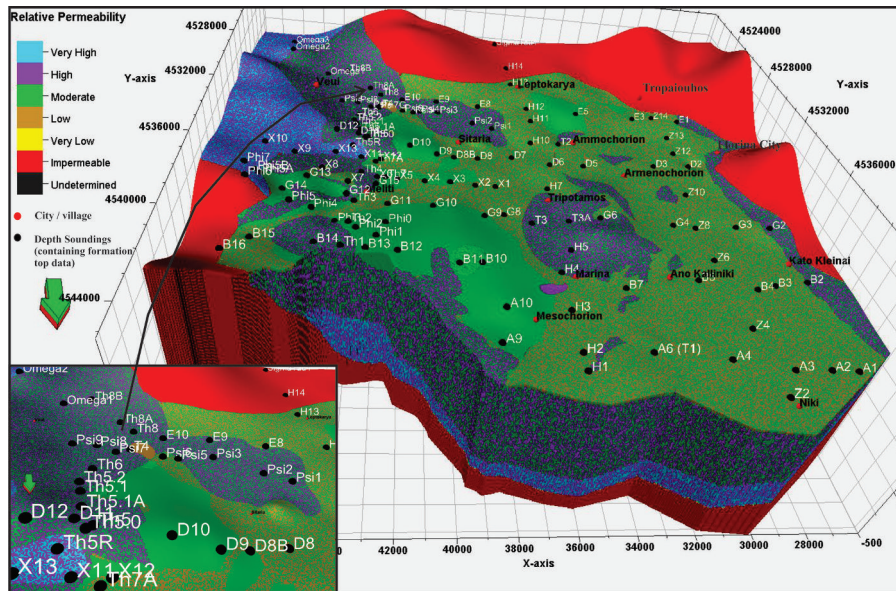


Figure 7: 3D view of the relative permeability model for the study area (view from the north) with positions of the electromagnetic depth soundings.

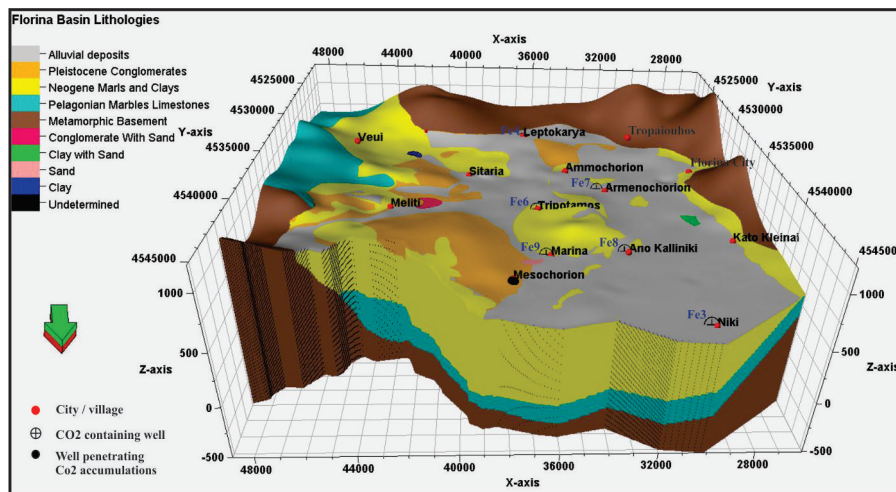


Figure 8: 3D view of the lithological model for the study area (view from the north) with positions of wells either penetrating through CO₂ accumulations or containing CO₂.

Table 1: Formation tops detected by the geo-electrical soundings and recorded in the database.

Formation Tops						
Clay with sand 1	Clay with sand 2	Clay with sand X	Clay with sand X	Crystalline Schist	Crystalline Schist Y	Crystalline Schist 1a
Clay 1	Clay 2	Clay 1a	Clay 3a	Marl 1	Limestone 1	Limestone 1
Sand X	Sand Y	Sand 2	Sand M1	Sand K1	Sand 1	Sand 1
Conglomerate 1b	Conglomerate 1	Conglomerate 2	Conglomerate with sand 1	Conglomerate with sand 3	Ground level	Ground level

(marls and clays), Pleistocene conglomerates and alluvial deposits (Figures 7 and 8).

We used the following 6 surfaces to build the 5-zone model, in order from shallow to deep (Table 3): the ground surface, the Pleistocene top surface, the Neogene top surface, the Pelagonian Nappe top surface, the metamorphic basement top surface and a base surface for the model set at -500 m depth (Table 3). We obtained these 6 surfaces by regrouping the formation tops previously described (Table 1) in order to obtain new combined surfaces that correspond to the upper limits of geological epochs or periods (Table 3).

A step of manipulating the above 6 surfaces (Table 3) was necessary in order to eliminate any parts that did not make sense geologically or that did not correspond to the data from the depth soundings. Once we obtained the treated surfaces with Petrel, we used supplementary functions in Petrel in order to construct the models. We first constructed a structural model describing the main rock boundaries and then defined a three-dimensional mesh honouring the structural model. This gave rise to the 5-zone model described above. We also incorporated lenses of various lithological compositions, whether they were made of clay, sand, clay with sand or conglomerate with sand using the corresponding formation tops (Table 1) and various lens-constructing techniques available in Petrel.

We chose to proceed with a simplification of the natural system through the construction of a 5-zone model due to the lack of seismic data and formation top data from wells. Since formation tops from electrical soundings were displayed in cross sections in paper format, it was impossible for us to interpret horizons in the usual way (i.e. using 2D or 3D seismic data).

Converting lithological boundaries in paper format, where boundary limits between electrical sounding measurements were often missing, into 3D boundaries across the basin in Petrel was technically demanding. In doing this exercise we extrapolated specific missing boundaries by following the inclination trend of the strata in the area. Another assumption we made was in the cases where the metamorphic basement was not recorded in the electrical soundings and was thus not recorded on paper. In these cases, if it made geological sense that the basement might exist at a certain depth where basement was not previously recorded, we marked it as present. In this manner we were able to interpret the top boundary of the basement across the whole study area.

The above interpretations allowed us to create a 3D model characterized by a maximum domain X width of 22,775 m and a maximum domain Y width of 24,075 m (Table 4). We chose these horizontal domain widths so

Table 2: Concentrations of free CO₂ and O₂ in the ground water at different locations. (For locations see Figures 8, 11–15.) [7]

Borehole	CO ₂ (mg/l)	O ₂ (mg/l)
FE3	132	0.35
FE4	30.8	2.19
FE6	118.8	0.36
FE7	2816	0.23
FE8	726	0.99
FE9	44	6

that the surface area covered by the model could cover the entire extent of the Florina Basin. The upper limit of the elevation depth range (1214.84 m) corresponded to the highest mountain peak in the area and the lower limit (-503.28 m) was deep enough to include at least the top of the metamorphic basement (Table 4).

Taking the above domain ranges into account, we then chose a small enough resolution for the grid that would capture the greatest detail possible without creating technical problems. From a technical point of view, models with a total 3D grid cell number in excess of several million cells are constructed with difficulty by Petrel. By choosing the above domain ranges and a 25 m by 25 m horizontal grid resolution, we created a model containing 52.6 million 3D grid cells (Table 4), thus avoiding software difficulties. Any finer horizontal grid resolution could not be applied as it would have technically prevented Petrel software from creating a model.

3.2.2 Model description

Once we created the 3D model grid (Table 4), we populated it with properties such as lithology according to the template in Table 5, which was made to take into account the lithology of the study area (Table 6). We also populated the 3D model grid with relative permeability derived from the hydrogeological map 5 – I from the preliminary hydrogeological study of the Florina area in 1975 (Figure 4) [7]. The relative permeability discrete values that we applied were converted to Petrel-readable codes according to the template in Table 6. Applying these codes is important for creating permeability contours and thus understanding how permeability is distributed in 2D (see results section below).

We then attributed a relative permeability value to each one of the zones and lenses of the model based on the indications from the hydrogeological map (Figure 4) [7]. The large variation in lithology that may exist within

Table 3: Regrouping of formation tops.

Surface used for constructing the model	Formation Top incorporation
Ground surface	ground surface
Pleistocene Top	clay with sand 2, sand 1, clay with sand 1, conglomerate with sand 1, conglomerate with sand 3
Neogene Top	marl 1, conglomerate 1, conglomerate 2, clay 1 and clay 2.
Pelagonian Nappe Top	limestone 1
Metamorphic basement Top	crystalline schist
Base surface	base surface

one of the 5 zones or lenses signifies that a range of relative permeability should be applied for this specific zone or lens when populating the models. For a summary of the relative permeability values attributed to the various zones and lenses found within these zones, see Table 7 below.

We used the map of isobaths of the aquifer background and of the equal thickness strata of the Neogene Group in which the aquifers are located (Figures 9 and 10) to construct isobath surfaces. We then applied the same templates for lithology and relative permeability as before (Tables 5 and 6). We used these isobath surfaces, especially the upper and lower limits for the Neogene Group to better understand the groundwater movement in the near surface and any links that may exist between ground water movement and CO₂ flow.

4 Results

4.1 Geological and sedimentological elements of the basin

A close look at the geological models we created show that the total thickness of the sediments above the metamorphic basement varies spatially (Figures 11–15). As we go from south to north, we observe that the basin becomes deeper and the sediments deposited there become much thicker (Figures 12–15). All cross sections show that the area around Mesochorion village contains the thickest deposits (located approximately 7 km to the SE of Mesochorion) (Figures 1, 8 and 11) where according to the model, we estimate up to approximately 1000 m of sediments are deposited above the basement. This thickness coincides with the maximum thickness proposed by previous research work [8, 21], thus reinforcing the accuracy of our newly-built model.

Once we entered the lithological boundaries and faulting into the lithological model (Figure 8), we were able to see how the metamorphic basement and other units outcrop at the surface and how they cover the entire 3D space. The metamorphic basement, for example, outcrops on the edges of the Florina Basin, especially on the south-western and north-eastern edges where the highest mountain peaks in the study area are also located (Figures 8, 11–15). Using the 3D lithological model, we were able to follow the morphology of the basement throughout the basin. The basement follows the form of a perfect curve very often (e.g. see curvature of the basement from Florina city towards Mesochorion [Figure 15]), but in most cases it is characterised by horsts and grabens (Figures 11–14).

According to our models, the thin semi-crystalline limestones and marbles of the Pelagonian Nappe mostly outcrop on the eastern side of the lithological model (Figures 8 and 13). We see the Pelagonian Nappe (Figure 8) (view from the north) at depth both under the villages of Mesochorion and Niki (Figures 8 and 11). Its thickness remains fairly constant between these two villages; it measures 250 m thick at Niki and 200 m thick at Mesochorion, but increases south-eastwards and south-westwards from Mesochorion (Figures 8, 10, 12 and 14). In the first case it reaches a thickness of up to 500 m (Figure 11), whereas in the second case, south of Armenochorion, its thickness can reach 470 m (Figure 12) to 510 m (Figure 14). The Pelagonian Nappe does not outcrop on the NW part of the study area but comes very close to the surface (Figure 8).

The construction of basin-wide models allowed us to also estimate the total rock volume of each of the zones in the models. We estimated, for example, that the Neogene marls and clays cover by far the biggest volume in the basin (i.e. 136.4 km³) within the limits of the study area (Table 8). The Neogene Group also outcrops in some locations in the centre of the basin, such as around Tripotamos village (Figure 8) and on the western edges of the

Table 4: Summary table of various model characteristics. (See also Figures 7 and 8.)

Model characteristics	
Min to Max X	26050 to 48825
Maximum Domain X width (m)	22775
Min to Max Y	4521150 and 4545225
Maximum Domain Y width (m)	24075
Area covered by model	$\approx 487\,204\,000\text{ m}^2 \approx 487.2\text{ km}^2$
Elevation depth range (m)	-503.28 to 1214.84
Grid cells ($nI \times nJ \times n\text{Grid layers}$)	$911 \times 963 \times 60$
Total number of 3D grid cells	52637580
Number of geological layers	60
Average Xinc (m)	25
Average Yinc (m)	25
Average Zinc (m) (along pillar)	20

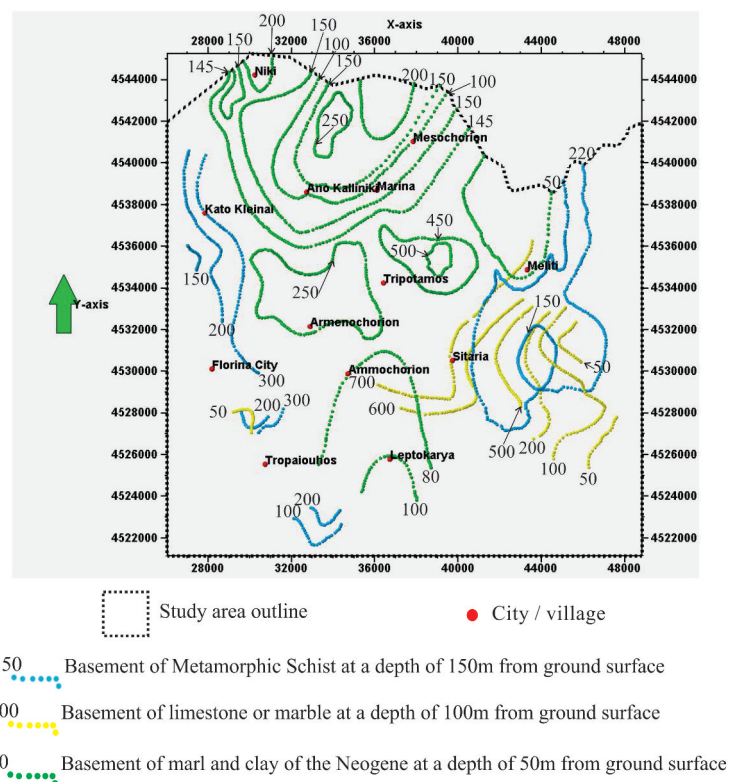


Figure 9: Map of isobaths of the aquifer in the Florina Basin.

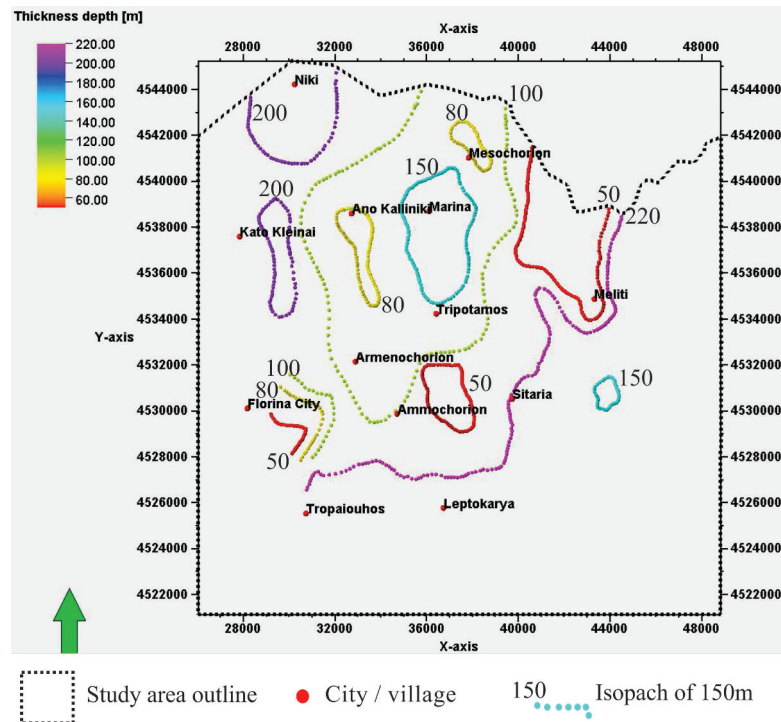


Figure 10: Map of equal thickness strata of the Neogene Group in which aquifers are located.

basin (e.g. around Florina city [Figures 8 and 15] and nearly around Tropaiouhos village [Figure 14]), where we observed a direct contact between the metamorphic basement and the Neogene Group without any Pelagonian marbles outcropping in between (Figure 15). We also observed this Neogene/metamorphic basement contact in the NE of the study area (Figure 15) and to the SE of Mesochorion village, where this contact is followed over a vertical distance of 700 m.

It is in this Neogene Group that we also located the CO₂ accumulations of the Mesochorion area (Figures 11, 13–15). Boreholes FE3, FE7, FE8 and FE9 penetrate through the Neogene group and FE6 and FE9 are located in areas where Neogene sediments outcrop (Figures 8, 14 and 15). There are surface indications of CO₂ seepage around Florina (Figure 15). From our geological models we see that this seepage occurs in an area where Neogene marls and clays outcrop at the surface but also where the basin is much shallower than in the rest of the study area; the metamorphic basement top at this location is about 150 m below the surface (Figure 15).

We found the Pleistocene conglomerates outcropping mainly at the NE of the study area near the villages of Meliti and Mesochorion (Figure 8). There is also another outcrop of Pleistocene conglomerates between Ammochorion and Leptokarya (Figure 8). In most cross sections these Pleistocene conglomerates correspond to superficial sediments

covering the uppermost layers of the subsurface, but the models showed that in some locations some deposits are more voluminous (e.g. at Mesochorion, 5 km to the SE of Mesochorion [Figure 11] and to the NW of Meliti [Figure 13]).

The alluvial deposits of the Holocene are mainly found in the central parts of the basin (Figure 8) but extend all the way to the northern edge of the model (Figure 8). A corridor of alluvial deposits is also developing just to the north of Meliti, where the fluvial deposits of the river go through Meliti (Figure 8). We estimated the thickness of the alluvial deposits and from the models they reach, at most, around 5 m in any part of the study area (see thin alluvial layer in Figures 7, 8, 11–15).

4.2 Description of the CO₂ geological reservoir

The CO₂ accumulations corresponding to the CO₂ geological reservoir that we encountered in the Mesochorion area are located in the Neogene marls and clays, between depths of 296–338 m and 380–409 m (Figures 11 and 13–15) [16]. The Neogene sediments in the Mesochorion area of the basin are characterized by deposits that we estimate to be ~700 m thick (Figures 11 and 13–15). The CO₂ accumulations are located somewhere in this Neogene Group, sug-

Table 5: Florina Basin lithology template.

Code	Lithology
0	Alluvial deposits
1	Pleistocene conglomerates
2	Neogene marls and clays
3	Pelagonian marbles and limestones
4	Metamorphic basement
5	Conglomerate with sand
6	Clay with sand
7	Sand
8	Clay
9	Undetermined

gesting an age of formation younger than Early Pliocene. The sediments around the reservoir are of moderate to high permeability (Figures 11 and 13–15). To the NW of these CO₂ accumulations lies a highly permeable sand lens (Figures 11 and 13–15). At the surface where the Mesochorion borehole is found, moderately permeable Pleistocene conglomerates outcrop (Figures 11 and 13–15).

We estimated the lower boundary of the aquifer that is located within the Neogene Group to be around 500 m depth, which is approximately 200 m above the top part of the CO₂ accumulations (Figures 11 and 13–15). The top part of the aquifer reaches ground level in the area and groundwater movement is generally towards the north (Figures 11 and 13–15).

We also encountered CO₂ accumulations at 3 different levels in the Meliti-Achlada area [27] but since we are unaware of the exact location of these accumulations, they will not be further considered in this paper for determining fluid flow pathways.

4.3 Structural characterization

The metamorphic basement is characterized by near vertical faults that are either normal (Figures 11 and 15) or reverse (Figure 13). Some of the crystalline rocks show faults with strikes oriented NE to SW. We also observed faults of NNE to SSW orientation at the eastern floor of the mountains.

Some of these near vertical faults reach the surface (see SE edge of cross sections in Figure 11). We also observed faults developing within the Neogene sediments (see area to the SE of Mesochorion, [Figure 11], below Armenochorion, [Figures 12 and 14] and below Meliti, [Figure 13]). In most of these cases their extent within the Neogene Group is limited, but the vertical fault developing

near Armenochorion (Figures 12 and 14) extends through the entire thickness of the Neogene sediments. This suggests a certain homogeneity in these sediments, at least in the area around Armenochorion and borehole FE7 (Figures 12 and 14).

Some of the normal faults that exist in the Neogene sediments develop also at the top of this model zone and into the overlying conglomerates (Figures 11 and 13). The conglomerates are deposited on the downward shifted side of the faults (Figures 11 and 13), and on the other side the Neogene sediments reach the surface. This could suggest that these faults have been responsible for creating the accommodation space for the younger Pleistocene sediments.

In some cases the faults continued further below and reached the Pelagonian limestones (see area SE of Mesochorion [Figure 11] and near Tropaiouhos [Figure 14]). In some cases where there is absence of the Pelagonian Nappe and the Neogene Group comes into direct contact with the metamorphic basement, we observed faults developing across the Neogene/Metamorphic basement contact (see area to the NE of Florina, Figure 15). This suggests that these faults were created during or after basin fill as they affect both the infill and the basement in the same way. If the graben was formed in Middle Tertiary age and the basin started to get filled in from the Late Miocene–Early Pliocene onwards, then these faults could not have been created before Late Miocene times.

There are normal faults located on the western margin of the study area in areas where the basement is much steeper than elsewhere (see area near Tropaiouhos, Figure 14, and near Florina, Figure 15). The faults can be followed all along the western margin of the basin. Normal movement of these faults could have led to the enlargement and deepening of the basin. Locally this can lead to more extreme deepening of the basin, such as could be the case between Tropaiouhos and Armenochorion (Figure 14), where the sediments filling the depression are much thicker than elsewhere.

4.4 Hydrogeochemistry

Although the water level during the dry period does not go deeper than about 10 m depth [7], in most of the locations where we recorded water appearance, the water level in aquifers in the basin could reach larger depths (Figures 9 and 10).

We focused our interest on determining in which sediments and at which depth groundwater flow is possible. The main interest is in the aquifer of the Neogene Group,

Table 6: Florina Basin relative permeability template.

Code	0	1	2	3	4	5	6
Relative Permeability	Very High	High	Moderate	Low	Very Low	Impermeable	Undetermined

as it is in these sediments that we encounter the CO₂ accumulations.

There is a general trend for groundwater in the Neogene sediments to flow from south to north and from the edges of the basin towards the centre (Figures 11–15). Between Mesochorion and Niki we hypothesized that groundwater could flow through the highly permeable sand lens located to the NW of Mesochorion and between 400–600 m depth (Figure 11). Near Niki and at the location of borehole FE3, the Neogene aquifer reaches ground level (Figure 11). To the SE of Mesochorion, the aquifer is very close to ground level, especially when moderately permeable lithology outcrops, such as the Pleistocene conglomerates (Figure 11).

Spatially, the development of the Neogene aquifer seems to follow the same general trend as the basin (i.e. where the basin deepens the Neogene aquifer also goes deeper and further away from the ground surface [Figures 11–15]) with the only exception being around the area of Mesochorion where the Neogene aquifer reaches the surface.

The hydrogeochemical survey of groundwater that was performed by the same company that carried out the rest of the study back in the 1970's [7] across the whole Florina Basin in order to determine if we could observe any changes in water chemistry in areas containing high CO₂ concentrations [1] gave the following results concerning the content of free CO₂ and O₂ in the ground water. These results, in conjunction with what we have presented up to now will allow us to discuss potential fluid flow pathways in the basin, especially in the Neogene sediments.

4.5 CO₂ leakage pathway identification in Florina Basin

CO₂ is a gas and does not necessarily flow using water as a medium. By looking at the relative permeability model and the location of faults in the region, we propose the following fluid migration pathways for CO₂ from the location of the Mesochorion geological reservoir in the north of the basin to other parts of the basin.

CO₂ could have flowed from the Mesochorion geological reservoir, located at approximately 300 m depth, to the near surface in several ways using different migration

pathways. From the map of isobaths of the aquifer background (see Figure 9) at Mesochorion, we can precisely locate the basement of the marls and clays of the Neogene at precisely 100 m depth. The thickness of the Neogene sediments at the Mesochorion well location reaches up to 720 m, meaning that below the depth of 100 m and down to the basement of the Neogene, CO₂ gas is free to move and will not be affected by the superficial water movement in the aquifer.

Water movement in the basin takes place towards the center and from south to north in the surface waters and aquifers of the basin. However, below the Neogene aquifer (i.e. below 100 m depth at Mesochorion) one can imagine CO₂ gas migrating laterally in all directions through the moderately to highly permeable Neogene sediments in order to reach, for example, Niki and borehole FE3 (Table 2 and Figure 11), Armenochorion and borehole FE7 (Table 2 and Figure 14), or even Florina city (Figure 15). CO₂ accumulations in the Mesochorion area are characterised by an absence of an upper cap rock layer [16]. CO₂ can therefore leak in these specific locations, not only laterally but also directly upwards.

Lenses of higher relative permeability (e.g. sand or conglomerate) that are scattered within the Neogene sediments also facilitate flow, such as in the case of the highly permeable sand lens located just to the south of Mesochorion that facilitates flow from Mesochorion to Armenochorion (Figure 14). If lenses are of lower permeability than the surrounding sediments (e.g. the conglomerate with sand lens between Meliti and Mesochorion [Figure 13]), CO₂ can flow around them. These lenses are small and surrounded by more permeable sediments within the aquifer so they will not block the pathway of CO₂.

Unsealed faults facilitate the migration of CO₂ as CO₂ and other fluids can use these discontinuities in the sediments in order to reach the surface. CO₂ migrating southwards from Mesochorion towards Marina and Armenochorion could have used the fault developing below the sand lenses and the vertical fault developing near FE7 (Figure 14) to flow laterally and upwards.

CO₂ under borehole FE7 is moving southwards, whereas ground water is moving northwards. Any CO₂ penetrating into the Neogene aquifer could be also drawn northwards away from FE7. The fact that the highest CO₂ levels are recorded at borehole FE7 may be linked to the

vertical fault developing there that would facilitate vertical migration of CO₂ and thus lead to high CO₂ readings in the groundwater.

4.6 Key processes controlling leakage of CO₂ in Florina

The boreholes showing the highest content of free CO₂ in the ground water are located near rivers as shown by the map of the points of electrical sounding (Figure 7) [7]. The flow of both surface water and ground water is towards the center of the basin and generally moves in a south to north direction, going also through the above mentioned boreholes (see hydrogeological map, Figure 4) [7].

CO₂ could have flowed from the location of CO₂ accumulations in the Mesochorion reservoir located at around 300 m depth to the rest of the basin via different processes. In Florina there is evidence of CO₂ having reached the surface (Figures 5, 6 and 9). Also, the upper limit of the aquifer that is located in the Neogene sediments reaches the surface at the exact location where CO₂ is observed in the fields outside the city (Figure 9). This indicates that CO₂ does not only migrate through the pores of the sediments but also through the water. More evidence that CO₂ can be dissolved in water, flow within it, and reach the surface comes from the observations made in 1) the field off Florina and 2) elsewhere in the basin where pools of water and CO₂ have been created (Figures 5 and 6).

The high CO₂ content in the ground water measured at FE7 (2816.0 mg/l, see Table 2 above) could be explained by the presence of faulting. High levels of CO₂ are recorded here despite the fact that the superficial sediments around FE7 are of low to moderate relative permeability (Table 7) and there is an aquifer where groundwater is flowing in the opposite direction as CO₂. This could be explained by the fault present underneath FE7, which has probably allowed CO₂ to use it as a fluid flow pathway to reach the surface (Figure 14).

In the proximity of borehole FE7 there is a NE-SW trending fault going through most of the formations in the basin (Figure 14). At the location of borehole FE7, we have already noted that the superficial sediments are of low relative permeability, but the relative permeability of the underlying sediments increases with depth (Figure 14b). The faults developing in the Neogene sediments, especially the vertical fault to the southwest of Armenochorion (Figure 14), could facilitate the vertical migration of CO₂. The CO₂ could migrate via the fault from the non-aquifer zone of the Neogene (e.g. below 360-400 m depth at the location of Armenochorion, FE7 and the fault) into the aquifer zone

and above. The CO₂ could then migrate further up, reach the surface, and migrate northwards to reach FE7, thus explaining the high levels of CO₂ recorded there (Figure 14).

The Mesochorion-Niki cross section (Figure 11) is the only example where groundwater and CO₂ flow directions coincide (i.e. they both flow in a general south-north direction). Although one would think that this would facilitate CO₂ flow, only a modest 132 mg/l of CO₂ is recorded at FE3. This could be due to the large surface area that the Neogene aquifer covers in the Niki/FE3 location. CO₂ flow here might be less focused compared to what is taking place near FE7. In Niki (Figure 11) CO₂ gets more dissipated and diluted as the aquifer reaches ground level and covers a larger area. CO₂ could reach the surface at several points whereas in FE7, where the aquifer is at least at 200 m depth, fluid flow is more focused due to upward migration along the vertical fault.

We have shown how CO₂ can migrate from the CO₂ accumulations of the Mesochorion area at approximately 300 m depth and go through the Neogene aquifers and faults to reach the surface (Figures 11–15). The presence of CO₂ in or passage of CO₂ through aquifers raises questions regarding the height of the water column and how much the hydrostatic pressure would increase the trapping of gases in the sediments. Observations have shown that CO₂ has flowed through the aquifer and reached the surface (Figures 11, 14 and 15), thus suggesting that the hydrostatic pressure is not sufficient to completely trap CO₂ gas in the sediments.

5 Discussion

5.1 Comparison of leakage pathways and potential of leakage for various sites

Comparing and contrasting key processes controlling leakage pathways between Snøhvit and Florina requires us to 1) characterise the potential of leakage for the two sites, 2) compare the leakage scenarios and 3) understand and compare the risks related to both sites.

The Snøhvit gas field, discovered in 1984, is located in the Barents Sea (BS) in the central part of the Hammerfest Basin (HFB) at a water depth of 310-340 m [28]. The HFB is about 130 km off the coast of Finnmark (Figure 16) and contains approximately 5000 m of strata above the basement [17].

The Lower Jurassic Tubåen Formation (TbF) [17] is an important reservoir where CO₂ has been injected since 2008 [13]. The Stø Formation (SF), of Pliensbach–Bajocian

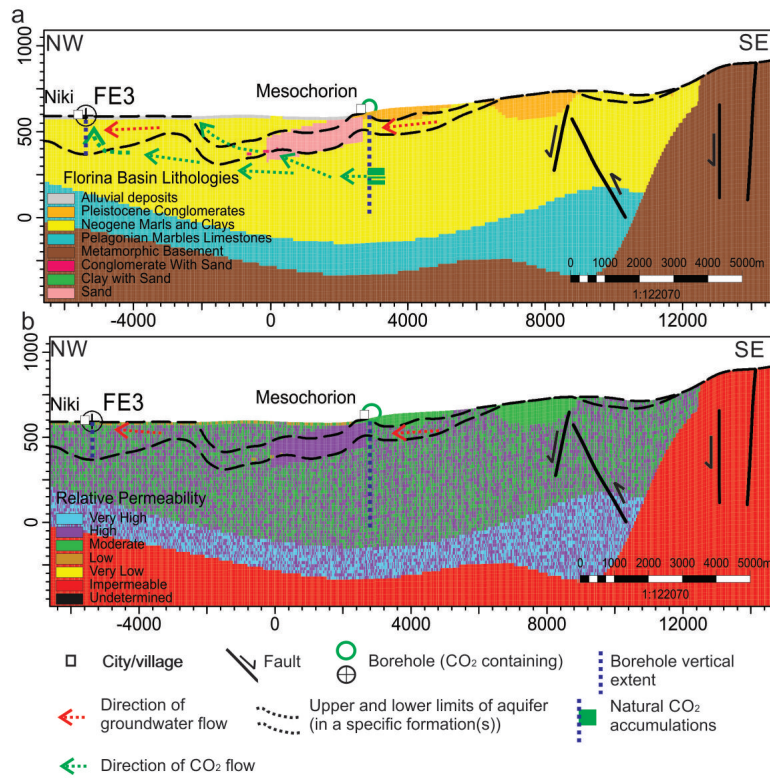


Figure 11: Cross section 1 passing through the villages of Niki and Mesochorion, showing a) lithology and b) relative permeability.

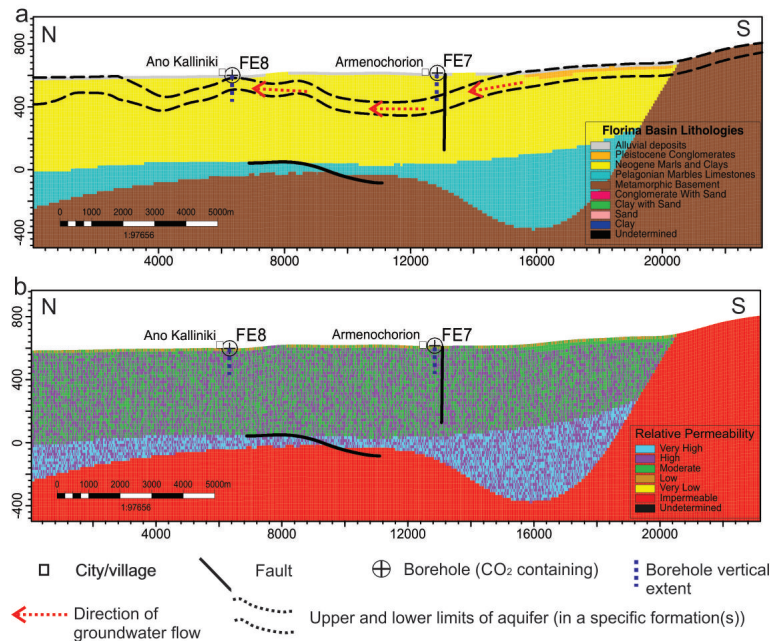


Figure 12: Cross section 2 passing through the villages of Ano Kalliniki and Armenochorion, showing a) lithology and b) relative permeability.

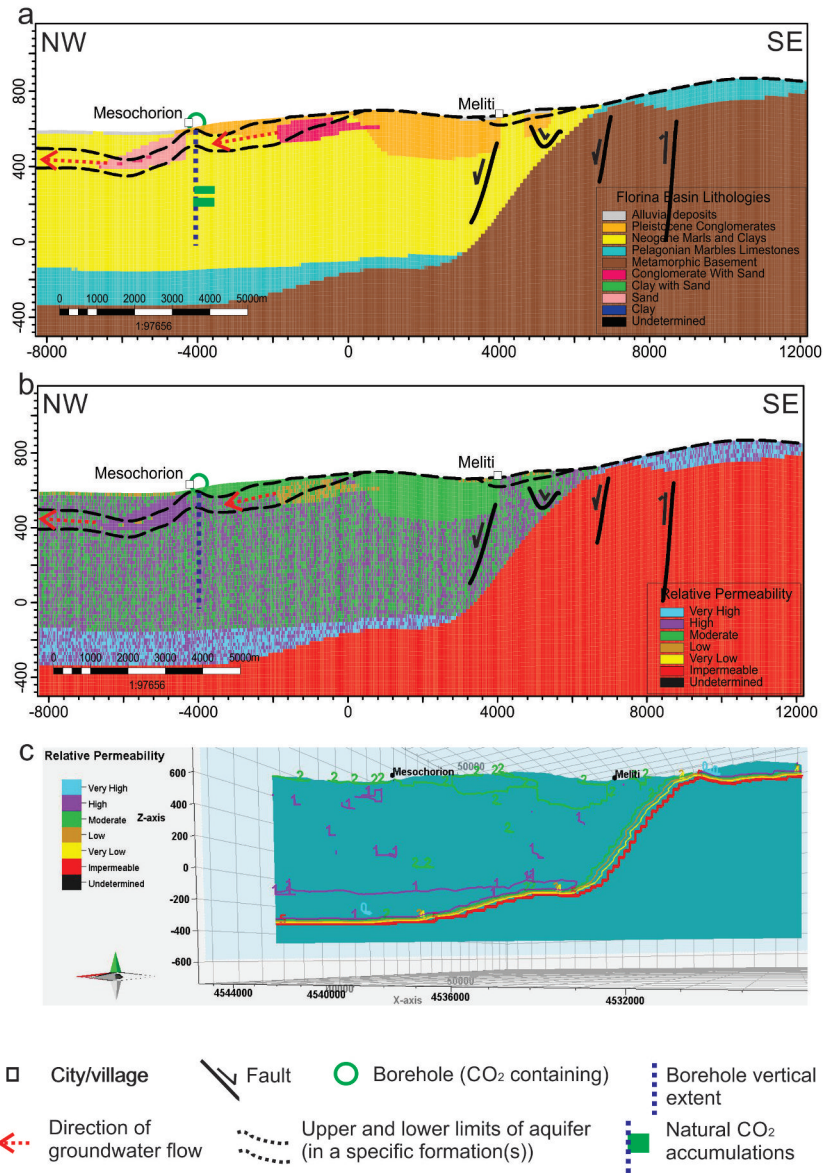


Figure 13: Cross section 3 passing through the villages of Meliti and Armenochorion, showing a) lithology, b) relative permeability and c) relative permeability contour values.

Table 7: Summary Table of the relative permeabilities used for the various lithologies.

Formation or lens	Relative Permeability range
Alluvials (Holocene deposits)	Low to Moderate
Pleistocene conglomerates	Moderate
Neogene	Moderate to High
Pelagonian Nappe	High to Very High
Metamorphic Basement: crystalline schists	Impermeable
Clay lens	Low
Sand lens	High
Clay with sand lens	Low to Moderate
Conglomerate lens	Moderate to High

Table 8: Estimated volume, using Petrel software, for some of the modeled zones.

Formation	Volume (km ³)	% Volume (%)
Alluvial deposits	2.52	1.35
Pleistocene conglomerates	10.47	5.62
Neogene marls	136.4	73.28
Pelagonian Nappe	36.75	19.74
TOTAL	186.14	100

age, is also an important reservoir rock of the HFB [17], consisting of vertically stacked units of lower to upper beach slope deposits [29].

Whereas at Florina the CO₂ source is shallow so the migration is only over a few hundred meters, at Snøhvit, the migration is over a few kilometers. Therefore, different distances and time scales are involved when considering the time it takes for CO₂ to potentially reach the surface.

At Florina, present-day seepage is observed at the ground level, but present-day seepage is absent at Snøhvit. This may be because there is still an active process allowing CO₂ to reach the top at Florina whereas at Snøhvit a deglaciation event which is no longer active led to fluid migration in the past [30].

Florina local cap rocks are comprised of clayey sediments [18]. Surface CO₂ seeps in Florina occur in areas where Tertiary clays and silt cover do not exist. At Snøhvit, leakage occurred at spill points located on or near faults and often in areas characterized by thin or absent cap rock. At Snøhvit the Hekkingen cap rock is composed of Upper Jurassic shales that are very organic-rich in the upper part [17]. The composition of the cap rock in the two sites is thus very similar and therefore expected to behave similarly.

The CO₂ reservoir in Florina is located at much shallower depths (i.e. around 300 m deep) than at Snøhvit. For both Snøhvit and Florina, faulting plays a key role in fluid migration. The fluid flow pathways between the two sites are comparable in nature (e.g. faults in both cases) but the

distance that fluids have to migrate is not comparable. At Snøhvit fluid has to flow through nearly 3 km [17] before it can reach the seabed.

The fluvial and alluvial fan environments located in the Florina Basin allow it to be used as a CO₂ storage site [16]. In fact, the internal change of stratigraphy in the same sedimentation environment acts as a barrier to leakage and does not allow the escape of CO₂ [16].

At Snøhvit there is currently no direct flow of gas from the Stør or Tubåen reservoirs to the seabed, but previously it has taken place as evidenced by the presence of gas chimneys, pockmarks and high amplitude anomalies above faults. In Florina, we have seen that fluid uses the fault and fracture system to migrate until it reaches the water table. This process is also observed in the Latera Caldera in Italy, where fluid migration above the water table occurs via gas-phase advective or diffusive flow, or it dissolves into the groundwater and migrates laterally via groundwater flow [31].

Gas transmitting faults in the extinct Latera Caldera volcanic site in Italy are also considered to be the main migration route for CO₂ to the atmosphere, reaching the surface through spatially restricted gas vents [31, 32]. Gas migration is guided along discrete, high-permeability pathways within the faults and can change dramatically along the fault strike [32]. Like in Florina, the CO₂ that leaks to the surface is driven not only by the water-dominated system but also by the high heat flow presently in the area [31].

The gas migration pathways are influenced by the style of the high density fracture domain in the area, which can be of 3 types, each representing different stages of the normal faulting process and/or the distribution of deformation along strike [31]. In one of the types, the “fault network” deformation, fluid migrates to the surface from top to bottom using conduit structures created from the interconnecting planes of faults and fractures [31].

5.2 Origin of CO₂ and timescales of leakage and CO₂ flow

CO₂ originates mainly from crustal sources (carbonate rocks) but has also a minor (10%) mantle contribution probably associated with the volcanic activity in the Almopia area (Voras Mountain area, Greece) [33, 34]. In the Florina Basin, it is the carbon isotopic composition, ranging from -2.3 to 0.3‰ (vs. V-PDB), that indicates a deep (magmatic / hydrothermal) origin of CO₂ [33, 34] and the He isotopic composition (0.24-0.82 R/Ra) that reveals a small (2-10%) but significant mantle contribution.

Information on the timing of the initiation of CO₂ leakage in the area is not known and cannot be hypothesized from the geological model that we built. However, we know that carbon dioxide occurs at various levels in the Mesozoic limestones and in overlying Neogene sandstones [10], therefore it could not have started to leak before the Mesozoic era.

Studies carried out in the extensive Almopia volcanic field (450 km³) [35] show that volcanic activity spanned the whole Pliocene. The older volcanic products are found at the Miocene-Pliocene boundary, and evidence of the last volcanic events are found at the Pliocene-Quaternary boundary, between 6.5 and 1.8 Ma [35]. Two large explosive events have also been dated: namely, the Xirorema Tephra formation (4.2 Ma) and the Papa Tephra formation (2.6 Ma). Since CO₂ flow seems to be associated with the above mentioned volcanic activity, we can hypothesize that CO₂ flow initiation could have taken place as early as 6.5 Ma and as late as 1.8 Ma.

We have seen previously that in the Florina Basin, CO₂ flow still takes place today (Table 2) and even reaches the surface (Figures 5, 6 and 15). Further evidence to support this observation comes from a study that examined soil gas CO₂ concentrations in the area near Florina city [36], where concentrations in some areas reach near 100% CO₂. Soil at the surface today can at places be saturated with CO₂ gas, suggesting that CO₂ flow reaches the surface. The distribution of the soil gas CO₂ concentrations is aligned along a NE-SW direction, similar to the direction of the ma-

ior faults in the area [36]. This suggests that the faults function at least in the present day as CO₂ flow pathways, allowing for localised leakage to take place at the surface.

At Florina, the upwards migration of CO₂ together with groundwater seems to be periodic. CO₂ concentrations vary substantially within the basin (Table 2) [37], reflecting the spatially and temporally variable flux of gas from depth. Hence, leakage may also be similarly spatially variable and episodic in rate [37].

If the episodicity in the rate of CO₂ leakage can be linked to the different episodes of volcanic activity in the area, then we have an idea of the periods when CO₂ leakage occurred and their duration. Volcanic activity occurred in three distinct magmatological and chronological periods. The first period occurred between 6.5 and 5 Ma, the second period between 4.9 and 4.2 Ma, and the third (and last) eruptive period between 4 and 1.8 Ma [35]. We could therefore assume 3 distinct CO₂ leakage episodes occurring during the above mentioned periods of volcanic activity, with durations of approximately 1.5 Ma, 0.7 Ma and 2.2 Ma, respectively.

5.3 Risk assessment

Commercial exploitation of CO₂ as an industrial gas started in the Florina Basin in 1980 and increased during the 1990s, with an average annual production of 20,000 t of CO₂ [23]. Annual production is currently around 30,000 tonnes of liquid CO₂ [18]. Around the same time (i.e. in 1984) production also commenced in Mc Elmo Dome, which is another analogue site in the U.S and the world's largest supply of commercially traded CO₂ [5]. It thus becomes important to deal with risk assessment in order to secure and improve the commercial exploitation of CO₂.

It has already been seen, such as in the case of the Latera Caldera in Italy, that gas release at the surface is primarily controlled by faults [31]. Risk assessment should thus emphasize determining the potential for and nature of CO₂ migration along permeable faults and fracture zones [6] since they can act as fast and direct conduits for CO₂ flow from the depth to the surface [6]. In the seismically active Florina Basin, seismicity can also play a role in influencing fluid migration as CO₂ leakage may be facilitated by earthquakes.

In the study area there are indications of CO₂ which has been dissolved in groundwater (see previous sections on surface indications of CO₂ at the surface near the city of Florina). CO₂ is thus dissolved in the groundwater of the existing Neogene aquifer, which reaches the surface around Florina city (Figure 15). In the case of a leak from

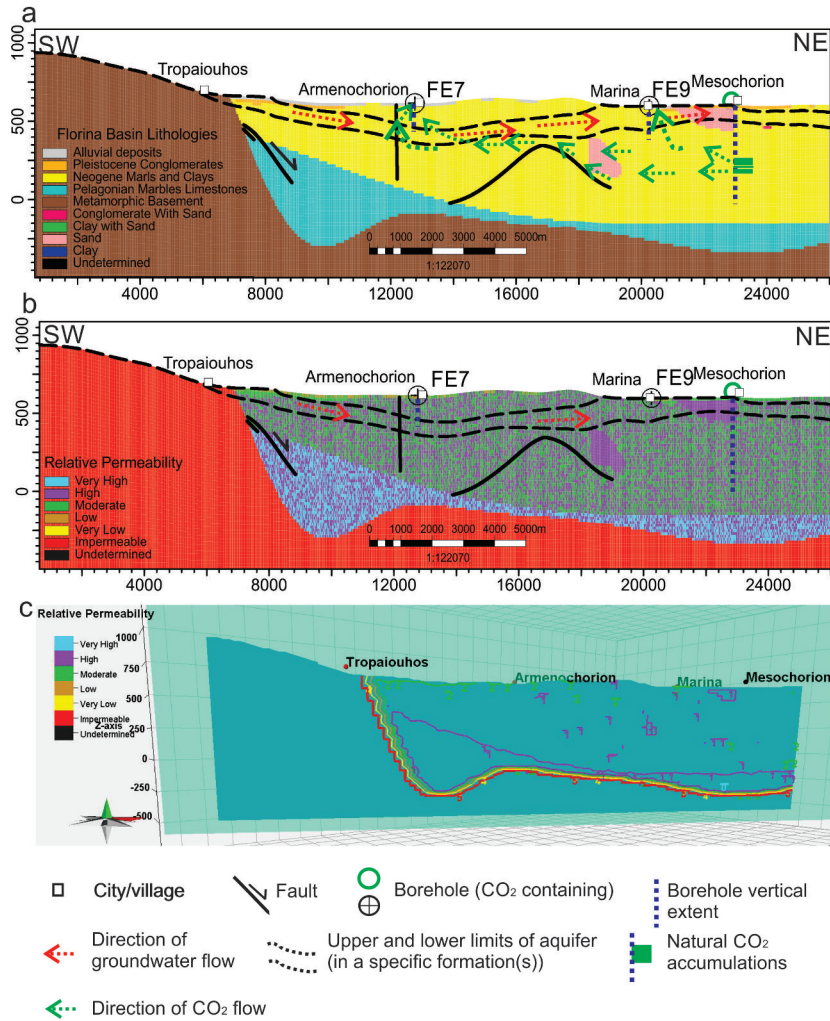


Figure 14: Cross section 4 passing through the villages of Mesochorion and Tropaiouhos, showing a) lithology, b) relative permeability and c) relative permeability contour values.

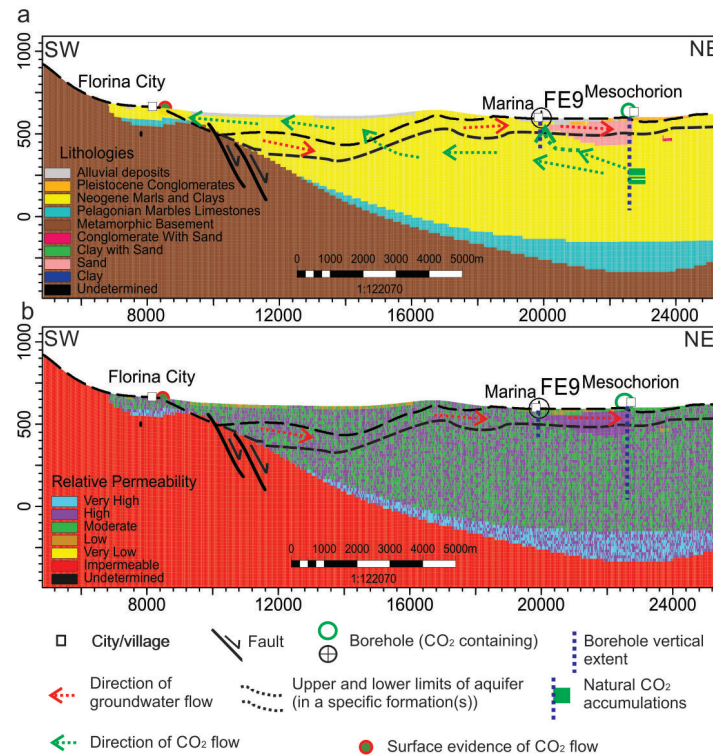


Figure 15: Cross section 5 passing through the villages of Mesochorion and ending in the city of Florina, showing a) lithology and b) relative permeability.

geological storage, we would also expect that CO_2 would be dissolved in water.

In relatively poorly consolidated successions, CO_2 leakage can be induced by drilling wells [10]. Wells may thus provide supplementary leakage pathways to the ground surface from natural CO_2 fields [10]. In such cases well drilling might pose a certain risk for health, as Florina is an inhabited terrestrial site. CO_2 can actually destroy wells, as has been seen previously, since increased CO_2 in the groundwater makes it acidic and consequently much more corrosive [10]. However, if adequate measures are applied, this risk, for both health and economy, is severely reduced as has been illustrated by the San Vittorino case study [1, 23].

In other parts of the world, such as in the Mc Elmo Dome site, an alarm system has been installed to warn people in case of CO_2 leakage [5]. In the first 15+ years of its operational history, no leakage has been recorded by the local community [5], thus illustrating that CO_2 storage can be monitored effectively.

In the Vorderrhon area in Germany, the installation of a continuous monitoring system over deep-seated fault systems, basalt intrusions, gaps in the overlying cap rock (salt beds) and former natural CO_2 production wells

showed no evidence of any leak [38], again suggesting that effective monitoring can reduce the risk of leakage to a minimum.

In the Latera Caldera in Italy, there is a possibility that the deep gas signature originating from the faults would be altered to some degree [31]. Such an alteration would influence the ability to locate CO_2 leakages (especially from buried faults) with any near surface monitoring technique [31]. This makes risk assessment a complicated matter which will have to take into account thickness, permeability, porosity, water content and chemistry of the unsaturated zone [31].

6 Conclusions

An analysis of the Florina natural analogue, through the development of geological models, has provided an estimate of the lithological composition and structure of the Florina Basin. More precisely, we have determined the zone thickness of each of the 5 zones in the model and their variation in space, as well as the relative permeability and lithological composition of each point in 3D space throughout the basin.

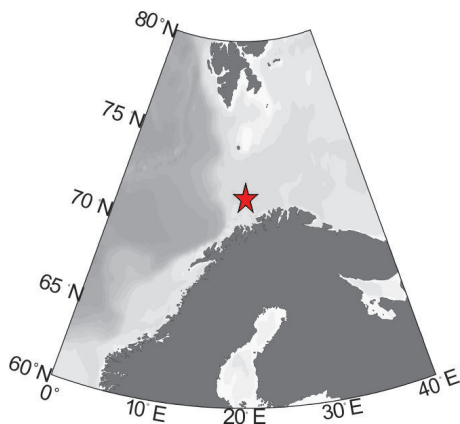


Figure 16: Location map of the Snøhvit field, SW Barents Sea, Norway.

The geological models that we built also allowed us to determine and visualise the potential pathways that CO₂ takes within the basin. They provided important insight into the lateral and vertical extent of the aquifer in specific formations throughout the basin by illustrating the basin-wide extent of the upper and lower limits of the aquifer. Finally, we have also determined through our model the possible directions of groundwater and CO₂ flow in the basin.

Northward the basin becomes deeper, specifically in the area around Mesochorion village where the thickest deposits occur. The geological model provided and confirmed the existence of around 1000 m of sediments above the basement in the area. The model also showed that the Neogene marls and clays cover by far the biggest volume in the basin: 136.4 km³ within the limits of the study area.

Geological faults developed during or after the creation of the basin. They affect both the Neogene sediments already deposited in the basin as well as the metamorphic basement. Permeable faults and fracture zones may act as conduits for CO₂ flow from depth to the surface. The surface indications of CO₂ seepage around Florina have also been observed in Neogene marls and clays, as shown by Figures 11–15 and the geological model. The faults developing in the Neogene sediments, for example, can facilitate the vertical migration of CO₂. Carbon dioxide accumulations in the Mesochorion area are characterised by an absence of an upper cap rock layer, as indicated by the model. CO₂ can therefore leak due to the absence of a cap rock in these specific locations, not only laterally but also directly upwards, as shown in Figures 11, 13–15.

CO₂ can flow 1) in the pores of the permeable sediments or 2) dissolved in water, either in the same direction or against the direction of groundwater flow. CO₂ could thus have flowed from the Mesochorion geological reservoir, located at approximately 300 m depth, through the

Neogene aquifers and faults to the near surface using several different migration pathways, as indicated in the geological model.

Developing a viable strategy to reduce the amount of greenhouse gases in the atmosphere, such as through CO₂ storage projects, is essential. Since CO₂ migrates through the shallow subsurface before it escapes to the atmosphere, understanding gas migration in the shallow subsurface is of the utmost importance. We accomplished this through the development of a localised geological model, which also allowed us to assess risk to human health and the environment.

The results from Florina site can form the basis for the development of novel monitoring techniques in future research. More specifically, we could undertake research activities that develop terrestrial leakage detection techniques and then compare them to monitoring strategies developed for seabed or sub-seabed leakage detection. The results from this research work can also be used as a basis to better understand CO₂ generation, migration and entrapment and give insight into the geochemical and mineralogical effects of carbon dioxide in the CO₂ natural analogue areas in Europe.

Acknowledgement: The authors are grateful to the technical team at Schlumberger, who developed the Petrel software which was used for the interpretation of data and the development of the geological models. The authors would like to thank the ECO₂ project and the Arctic University of Norway for providing the funding for carrying out parts of this piece of research. We would also like to thank both reviewers for the time they spent reviewing the manuscript and for their suggestions and insightful comments on the paper, as these comments have led to a significant improvement of the work and of the manuscript. Finally, we would also like to express our gratitude to the Language Editor, Cassidy Jay, for her suggestions and corrections.

References

- [1] Pearce J.M., What can we learn from natural analogues? - An overview of how analogues can benefit the geological storage of CO₂. *Advances in the Geological Storage of Carbon Dioxide: International Approaches to Reduce Anthropogenic Greenhouse Gas Emissions*, 2006, 65, 129–139.
- [2] Czernichowski-Lauriol I., Rochelle C., Lindeberg E., Bateman L., Sanjuan B., Analysis of the geochemical aspects of the underground disposal of CO₂. In: *Deep Injection Disposal of Hazardous and Industrial Waste: Scientific and Engineering Aspects*, J.A. Apps, C.F. Tsang (Eds.), Academic Press, London, UK, 1996. 565–585.

- [3] Pearce J.M., Holloway S., Wacker H., Nelis M.K., Rochelle C., Natural occurrences as analogues for the geological disposal of carbon dioxide. *Eng. Convers. Manage.*, 1996, 37(6-8), 1123–1128.
- [4] Stevens S.H., Fox C.E., Melzer L.S., McElmo Dome and St. Johns Natural CO₂ Fields: Analogs for Geologic Sequestration. Fifth International Greenhouse Gas Control Conference, 13-16 August, Cairns, Australia, 2000.
- [5] Stevens S.H., Pearce J.M., Rigg A.J., Natural Analogs for Geologic Storage of CO₂: An Integrated Global Research Program. First National Conference on Carbon Sequestration U.S. Department of Energy National Energy Technology Laboratory May 15-17, Washington, D.C, 2001.
- [6] Lewicki J.L., Birkholzer J., Tsang C.F., Natural and industrial analogues for leakage of CO₂ from storage reservoirs: identification of features, events, and processes and lessons learned. *Environ. Geol.*, 2006, 52, 457–467.
- [7] Ampas V., Hydrogeological study of the Florina region. Volume I : Hydrogeological Report. Hydrotechniki S.A., Athens, Greece, 1975. reservoirs: identification of features, events, and processes and lessons learned. *Environ. Geol.*, 2006, 52, 457–467.
- [8] Koukouzas N., Ziogou F., Gemeni V., Preliminary assessment of CO₂ geological storage opportunities in Greece. *Int. J. Greenhouse Gas Control*, 2009, 3(4), 502–513. reservoirs: identification of features, events, and processes and lessons learned. *Environ. Geol.*, 2006, 52, 457–467.
- [9] Gaus I., Le Guern C., Pauwels H., Girard J.P., Pearce J., Shepherd T., Hatziyannis G., Metaxas A., Comparison of long-term geochemical interactions at two natural CO₂-analogues : Montmiral (Southeast Basin, France) and Messokampos (Florina Basin, Greece) case studies. Proceedings of the 7th International Conference on Greenhouse Gas Control Technologies, Vancouver, Canada, 5-9 September, 2005. reservoirs: identification of features, events, and processes and lessons learned. *Environ. Geol.*, 2006, 52, 457–467.
- [10] Hatziyannis G., Arvanitis A., Natural analogues of CO₂ leakage in Florina area, Northern Greece. 2nd CGS Europe Knowledge Sharing Workshop on Natural Analogues, Maria Laach, Germany, 17-19 October, 2011. reservoirs: identification of features, events, and processes and lessons learned. *Environ. Geol.*, 2006, 52, 457–467.
- [11] Chiaramonte A., White J.A., Johnson S., Preliminary geomechanical analysis of CO₂ injection at Snøhvit, Norway. *American Rock Mechanics Association*, 2011, 11(441), 1–9. reservoirs: identification of features, events, and processes and lessons learned. *Environ. Geol.*, 2006, 52, 457–467.
- [12] Eiken O., Hansen O., Gilding D., Nazarian B., Osdal B., Ringrose P., Kristoffersen J.B., Hansen H., Snøhvit: The history of injecting and storing 1 Mt CO₂ in the fluvial Tubåen, Fm. *Proc. GHGT11*, 2013, 37, 3565–3573.
- [13] Maldal T., Tappel I.M., CO₂ underground storage for Snøhvit gas field development. *Energy*, 2004, 29(9 -10), 1403–1411.
- [14] Shi J.Q., Imrie C., Sinayuc C., Durucan S., Korre A., Eiken O., Snøhvit CO₂ storage project: Assessment of CO₂ injection performance through history matching of the injection well pressure over a 32-months period. *Energy Procedia*, 2013, 37, 3267–3274.
- [15] Vadakkepuliambatta S., Buenz S., Mienert J., Chand S., Distribution of subsurface fluid-flow systems in the SW Barents Sea. *Mar. Petrol. Geol.*, 2013, 43, 208–221.
- [16] Karakatsanis S., Koukouzas N., Pagonas M., Zelilidis A., Preliminary sedimentological results indicate a new detailed stratigraphy for the Florina sedimentary basin and relate them with CO₂ presence. *Bull. Geol. Soc. Greece. Proceedings of the 11 th International Congress, Athens, May, 2007, 2007. XXXX.*
- [17] Linjordet A., Olsen R.G., The Jurassic Snøhvit Gas-Field, Hammerfest Basin, Offshore Northern Norway. *Giant Oil and Gas Fields of the Decade 1978-1988*, 1992, 54, 349–370.
- [18] Baines S.J., Worden R.H., Geological storage of carbon dioxide. Geological Society special publication. Geological Society, London, Tulsa, OK, Distributed by AAPG Bookstore, 2004, 255.
- [19] Hatziyannis G., The role of Capture and Storage of CO₂ (C.C.S. - Capture and Storage of CO₂) when dealing with climate change. IENE Conference on Climate Change, Athens, Greece, 8th February, 2007.
- [20] Pavlides S.B., Neotectonic Evolution of the Florina-Vegoritida-Ptolemaida (Western Macedonia) basin. PhD thesis, Geological Faculty of the Aristotelian University of Thessaloniki, 1985.
- [21] Metaxas A., Karageorgiou D.E., Varvarousis G., Kotis T., Ploumidis M., Papanikolaou G., Geological evolution-stratigraphy of Florina, Ptolemaida, Kozani and Saradaporo Graben. Proceedings of the 11 International Congress, Athens, Bull. Geol. Soc. Greece 2007, XXX, 1409–1420.
- [22] Ziogou F., Gemeni V., Koukouzas N., de Angelis D., Libertini S., Beaubien S.E., Lombardi S., West J.M., Jones D.G., Coombs P., Barlow T.S., Gwosdz S., Krüger M., Potential environmental impacts of CO₂ leakage from the study of natural analogue sites in Europe. *Energy Procedia*, 2013, 37, 1–8.
- [23] Pearce J.M., Stevens S.H., Rigg A.J., Natural Analogs for Geologic Storage of CO₂: An Integrated Global Research Program. Washington, D.C., USA, 15-17 May, 2001.
- [24] Pavlides S.B., Mountrakis D.M., Extensional Tectonics of Northwestern Macedonia, Greece, since the Late Miocene. *JSG.*, 1987, 9(4), 385–392.
- [25] Steenbrink J., Hilgen F.J., Krijgsman W., Wijbrans J.R., Meulenkamp J.E., Late Miocene to Early Pliocene depositional history of the intramontane Florina-Ptolemais-Servia Basin, NW Greece: Interplay between orbital forcing and tectonics. *Palaeogeogr. Palaeoclimatol. Palaeoecol.*, 2006, 238(1-4), 151–178.
- [26] Gwosdz S., Jones D., West J.M., Coombs P., Green K., Gregory S., Smith K., Möller I., Ziogou F., Gemeni V., Krüger M., Impacts of elevated CO₂ concentrations on CO₂-adapted and non-adapted environments, Trondheim, Norway, 4-6 June, 2013.
- [27] Kotis T., Ploumidis M., Metaxas A., Varvarousis G., Exploration of lignite deposits in the eastern region of the Florina basin, subarea Meliti-Lofi. *I.G.M.E.*, 1996, Annex I, 1–91.
- [28] Hansen J.Ø., Rasen B., Facts 2012- The Norwegian Petroleum Sector. Annual Report, Norwegian Ministry of Petroleum and Energy and Norwegian Petroleum Directorate, Stavanger, Norway, 2012.
- [29] Worsley R.J., Edrich S.P., Hutchison I., The Mesozoic and Cenozoic succession of Tromsøflaket In: A Lithostratigraphic Scheme for the Mesozoic and Cenozoic Succession Offshore Mid- and Northern Norway. *Norwegian Petroleum Directorate Bulletin*, 1988, 4, 42–65.
- [30] Ostanin I., Anka Z., di Primio R., Hydrocarbon plumbing systems above the Snøhvit gas field: Structural control and implications for thermogenic methane leakage in the Hammerfest Basin, SW Barents Sea. *Mar. Petrol. Geol.*, 2013. 43, 127–146.

- [31] Annunziatellis A., Beaubien S.E., Bigi S., Ciotoli G., Coltella M., Lombardi S., Gas migration along fault systems and through the vadose zone in the Latera caldera (central Italy): Implications for CO₂ geological storage. *Int. J. Greenhouse Gas Con.*, 2008, 2(3), 353–372.
- [32] Arts R.J., Baradello L., Girard J.F., Kirby G., Lombardi S., Williamson P., Zaja A., Results of geophysical monitoring over a leaking natural analogue site in Italy. *GHGT-9*, 2009, 1(1), 2269–2276.
- [33] D'Alessandro W., Bellomo S., Brusca L., Elevated trace metals and REE contents in the CO₂-rich groundwaters of Florina (N. Greece) - A natural analogue of Carbon Storage Systems. Abstract, *GeoMed2011 - 4th International Conference on Medical Geology*, September 2011, Bari, Italy, 2011a.
- [34] D'Alessandro W., Brusca L., Kyriakopoulos K., Karakatsanis S., Groundwater quality issues in the Florina area (N. Greece). 26th European Conference - *SEGH 2008 Health Implications of Environmental Contamination*, 31 March - 2 April, 2008, Athens, Hellas, Poster presentation, 2008.
- [35] Vougioukalakis G.E., Petrological, geochemical and volcanological study of the pliocene volcanic formations of Almopia and their correlation with the geothermal manifestations in the area. PhD Thesis, Aristotele University of Thessaloniki, Geology Department., 2002, 382.
- [36] Beaubien S., Impacts on Groundwater. *RISCS Final Conference*, Rueil-Malmaison, France, November 2013.
- [37] Blackford J., Beaubien S., Foekema E., Gemeni V., Gwosdz S., Jones D., Kirk K., Lions J., Metcalfe R., Moni C., Smith K., Steven M., West J., Ziogou F., A guide to potential impacts of leakage from CO₂ storage. D5.2b, Revision: 5. *RISCS Consortium*, 2013.
- [38] Teschner M., Brune S., Faber E., Poggenburg J., Automatic gas-geochemical monitoring stations in the Vorderrhon region, Thuringia, Germany. In: *CO₂ Leakage mechanisms and migration in the ear-surface*. S.J. Kemp (Ed.), Final report, WP3, Nascent project, British Geological Survey Commissioned Report CR/03/196, 2004.